

# PERFORMING HIGHLY ACCURATE PREDICTIONS THROUGH CONVOLUTIONAL NETWORKS FOR ACTUAL TELECOMMUNICATION CHALLENGES

**Jaime Zaratiegui, Ana Montoro & Federico Castanedo**

Data Science Department

WiseAthena

San Francisco, CA, USA

{jaime.zaratiegui, ana.montoro, fcastanedo}@wiseathena.com

## ABSTRACT

We investigated how the application of deep learning, specifically the use of convolutional networks trained with GPUs, can help to build better predictive models in telecommunication business environments, and fill this gap. In particular, we focus on the non-trivial problem of predicting customer churn in telecommunication operators. Our model, called WiseNet, consists of a convolutional network and a novel encoding method that transforms customer activity data and Call Detail Records (CDRs) into images. Experimental evaluation with several machine learning classifiers supports the ability of WiseNet for learning features when using structured input data. For this type of telecommunication business problems, we found that WiseNet outperforms machine learning models with hand-crafted features, and does not require the labor-intensive step of feature engineering. Furthermore, the same model has been applied without retraining to a different market, achieving consistent results. This confirms the generalization property of WiseNet and the ability to extract useful representations.

## 1 INTRODUCTION

Advances in the amount of available data, hardware performance and methods for training deep learning networks (Hinton et al., 2006) (Srivastava et al., 2014) have shown an extraordinary predictive performance improvement in areas such as audio processing (Senior et al., 2013), image recognition (Simonyan & Zisserman, 2015) (Szegedy et al., 2014), natural language processing (Mikolov et al., 2013b) and video analysis (Simonyan & Zisserman, 2014) (Karpathy et al., 2014).

One of the strengths of deep learning networks is the ability of discovering hierarchical feature representations from large amount of input data by the composition of multiple non-linear transformations. Therefore the traditional step of building hand-crafted features (a.k.a. feature engineering) which is difficult, time consuming and requires domain knowledge, can be avoided by using deep learning (Bengio et al., 2013) and convolutional networks (ConvNets) in the specific case of images (LeCun et al., 2010). Motivated by the fact that these networks discover hierarchical representations from input data, we investigated their application to predict churn in prepaid telecommunication customers, and developed the WiseNet model.

Customer churn may be defined as the loss of a customer resulting from, for example, the customer switching to a competitor’s product or service. Predicting churn of prepaid telecommunication customers is a complex task since there is no specific termination date of their contract. In this circumstances, deactivation occurs after a period of time during which the customer did not perform a balance replenishment. It can be further observed that, once the customer has decided or is in the process of deciding whether to transition, the customer’s phone usage patterns may start to change. The sooner these changing patterns are detected, the more opportunities and time are available to the telecommunications service provider to try to retain the customer. Being able to predict which customers most likely stop their replenishment gives companies a competitive advantage to retain

customers since they can perform specific commercial to reduce the likelihood that the customer will churn. This problem has been approached by training binary classifiers with the behavior of known churners/non-churners and then applying the trained model to predict future behaviors. Previous state-of-the-art works tackled the problem by training machine learning models with hand-crafted features (Huang et al., 2012) (Luciano et al., 2015) (Wilson et al., 2015) (Yoon et al., 2010) (Burez & Van den Poel, 2009b) or by applying social network analysis (Richter et al., 2010).

Whereas the superiority of ConvNets against traditional machine learning models is clear when dealing with noisy unstructured data (e.g. images), their application to structured input data has been less explored. In this article, we show that the application of ConvNets using structured data outperforms traditional supervised classifiers with hand-crafted features, with no the need to perform the labor-intensive step of feature engineering. To the best of our knowledge, this is the first work which provides an exhaustive comparison between feature-engineering machine learning models, and ConvNets using structured data for a real business problem.

Our main contributions are the following:

- The development of a novel method to encode customer behavior into images specifically crafted for applying structured data from a real telecommunication business problem to WiseNet.
- An experimental evaluation with different machine learning models showing the ability of WiseNet to learn features when dealing with structured data.
- A comparison with a production system developed using hand-crafted features showing the advantage of WiseNet in this problem.
- The application of the same network architecture, weights and hyperparameters to a different market without retraining, showing the generalization and transfer learning property of the WiseNet model.

In more detail, our findings are described as follows; in the next section we provide details about the type of data we deal with and the approach to encode customer behavior into images. Then the WiseNet network architecture employed to solve this problem is discussed (Section 3) and experimental results using WiseNet and machine learning classifiers over the same datasets are given in Section 4. Finally, the conclusions of this work are shown in Section 5.

## 2 DATA REPRESENTATION

In a telecommunication environment, several data sources are available from the customer behavior point of view, such as Call Detail Records (CDRs), balance replenishment events (topups), geographical activity, social network activity, data-usage behavior, promotions/marketing campaigns, to name a few. In order to come up with a general model our goal is to avoid specific details and therefore use the least and rawest data as possible. In this work, we only use the following data from the customer behavior:

- Call Detail Records (CDRs): providing log information with details about each call made by the customer. This information includes the cell tower where the call was made, the number originating the call<sup>1</sup>, when the call was made (time-stamp), the duration of the call, the destination number, and the service identification (incoming/outgoing call or sms).
- Topups: describing a history of balance replenishment events for each customer, basically the customer-id, the time-stamp and the amount spent.

We were motivated to employ these pieces of data seen the impressive results of ConvNets, from among the myriad of deep learning architectures. The basics of ConvNets are template layers slides which are learned during training on the image pixels. Therefore, we need to encode customer behavior data into artificial images. This encoding step can be seen as a transformation from the input space to a specific training domain, similarly to what is done with word representations in the word2vec model (Mikolov et al., 2013a).

<sup>1</sup>To enforce security and privacy issues the destination and originating number are always encrypted.

## 2.1 IMAGE ENCODING

In our work, customer data is encoded into a linear time representation. Hence, time is linearly mapped into the  $x$ -axis of the image. The  $y$ -axis is reserved for each one of the data sources, i.e. outgoing call activity (MOC), incoming calls (MTC) and topups.

The image width spans the whole period of time we considered in the training stage, which is exactly four weeks or 28 continuous days of user activity. Furthermore, we have split each day into 12 equally sized time slices and and, as a result, each of these slices, i.e. pixels, spans a period of two hours. Therefore, the total image width and height in pixels is  $336 \times 3$ .

The value or intensity of each pixel in the image is proportional to the customer’s activity in each of the three possible categories. For example, let us assume a customer has a 20 minute outgoing call in a certain time slice  $t_n$ , the base value for that pixel would then be  $20/120 = 1/6$ , as 120 minutes is the maximum activity that can be registered. Due to the fact that most variance is found closest to zero activity, we scale the pixel’s base value  $I$  according to the following power law

$$I(k, t_n) = I_{kn}^\alpha, \quad (1)$$

where  $t_n$  is the  $n$  time slice and  $k$  is a categorical label that indicates either outgoing or incoming calls and  $\alpha$  is chosen to be equal to  $1/7$  in order to better exploit variance in those pixels that have the lowest base values. Continuing with the example of a 20 minute outgoing call, we would finally have that the normalized value of the pixel will be  $I = 6^{-1/7} = 0.774$ , which in an 8-bit image corresponds to the pixel value 197. We have chosen each of the RGB channels to represent separately each of the three categories MOC (red), MTC (green) and topups (blue), as shown in Figure 1.

For the topup activity channel, we have chosen a different way of representing the input data. In this case, the balance topup activity is predominantly done by redeeming coupons of discrete value and seldom by doing a bank transfer of a non-preset quantity. Consequently, the pixel values will be mostly discrete. In this case, the pixel intensity will be linearly proportional to the amount replenished but will saturate at a certain point. We have set as saturation value the maximum value of a single prepaid coupon which is available for purchase. Of course, a single customer could redeem several of these maximum face value coupons in the same two hour period but the value of that pixel in the blue channel will not be affected as it will already be saturated.

A single extra feature has been added to the images, that is a white  $1 \times 3$  pixel mark at each point where local time is Monday at 00:00 hours. This is done at the expense of all activity data at that point as the white vertical stripe deletes any previous value present at that point. The purpose of this stripe is identifying the weekly periodicity inherent to calendar days besides any other recurring activity that the user could have (see Figure 2).

Each of the images is labeled according to the user topup activity in the 28 consecutive days following to the training data shown in the image. Churners are defined as those who did not have any topup activity in this period and therefore, their corresponding images are labeled as 1.



Figure 1: Different pixel categories and intensity range in the RGB scale for each one of the customer events. The size of a 2-hour pixel is delimited by the gray arrows. The vertical arrangement of the three data categories MOC/MTC/topups is kept equal in all images.



Figure 2: An encoding example of a nine day period for a single customer with a high degree of activity in the three categories. Start of the week white mark can be observed in the middle of the image. Time increases from left to right.

In order to train and validate the models we followed a standard train, test and validation data partitioning. We took a sample of 132.779 different customers in a three-month period from January

2015 till end of March 2015. The four week training period is taken at random within the available time span, given the condition that there is enough data for the additional 28 days required for labeling the image. The train set was composed of 102K customers, test set of 18K and validation set of 37K different customer instances. The test set was used to tune the classifiers' optimal parameters such as number of neurons, depth of the hidden layers or learning rate. The performance metrics of the classifier such as AUC or logarithmic loss, are evaluated using the validation set.

### 3 NETWORK ARCHITECTURE

As we have mentioned before, to develop the WiseNet architecture, we selected ConvNets due to their ability to generalize to new samples and to perform feature learning. ConvNets have a specialized connectivity structure which exploits the strong spatial correlation exhibited in the customer-behavior artificial images. Another reason for using convolutions is that our patterns may be shifted around and it would be desirable to detect this based on the position in the image.

Once features are learned using ConvNets, they are passed to a fully connected neural network which combines them in order to classify the input image into one specific class. In our case, images represent customers' behavior and the target class indicates if they are active or inactive customers (churners).

We used pooling layers and experimented with different network architectures, activation functions and initialization procedures. We found that networks are remarkably sensitive to the initialization and the activation functions.

ConvNets with pooling layers have some translation invariance built into their architecture. A pooling layer summarizes the information of the convolution units in a smaller number of units. A unit in a pooling layer receives input from a small neighborhood of convolution units in the layer below. Pooling layers can be divided into sum, average or max pooling. We use max-pooling layers, which means that the strongest convolutional filter response in the small region is passed on to the next layer.

It has been shown that a standard gradient descent performs poorly with random initializations in deep neural networks. Glorot and Bengio proposed a new initialization scheme that provides faster convergence (Glorot & Bengio, 2010). They demonstrated that the normalization factor may be important when deep networks are initialized because of the multiplicative effect through layers. To maintain activation variance and back-propagated gradient variance as ones moves up or down the network, they proposed the following normalized initialization:

$$W \sim U \left[ -\frac{\sqrt{6}}{\sqrt{n_j + n_{j+1}}}, \frac{\sqrt{6}}{\sqrt{n_j + n_{j+1}}} \right] \quad (2)$$

One of the benefits of this initialization procedure is to hold gradients of similar magnitudes at different layers and therefore to have the effect of a faster training. We employed this initialization procedure in the fully connected layers.

Regarding activation functions, we used parametric rectifier linear units (PReLU) (He et al., 2015). This type of activation function simplifies backpropagation, makes the learning phase faster and avoids saturation issues.

The design of the architecture of the network can be split into two stages or modules. In the first stage, convolutional and spatial pooling layers are applied sequentially taking as inputs the set of  $336 \times 3$  RGB images. In the second stage, a series of fully connected hidden layers are used with the objective of exploiting the features extracted in the first stage.

The convolution filters used in the ConvNet are relatively small. In the first hidden layer, we have used a rectangular  $6 \times 1$  kernel with a stride of 1. In this step, using a 1-pixel high filter, we aim to extract features which are dependent only on each of the rows of the images, i.e. the three different activity categories will not be mixed in this operation. After the second convolution layer, the data from the three rows of the image will be mixed as we are using a  $6 \times 3$  filter. The width of the convolution layers is also quite small, just 32 channels wide. The exact specifications of the WiseNet are shown in Table 1 and a visual illustration of the architecture is represented in Figure 3.

| Layer         | dim            | channels | kernel       | stride |
|---------------|----------------|----------|--------------|--------|
| Input RGB     | $336 \times 3$ | 3        |              |        |
| Convolutional | $331 \times 3$ | 32       | $6 \times 1$ | 1      |
| Max Pooling   | $326 \times 3$ | 32       | $6 \times 1$ | 1      |
| Convolutional | $321 \times 3$ | 32       | $6 \times 3$ | 1      |
| Max Pooling   | $161 \times 3$ | 32       | $2 \times 1$ | 2      |
| FC-512        |                |          |              |        |
| FC-512        |                |          |              |        |
| FC-1024       |                |          |              |        |
| FC-2          |                |          |              |        |
| soft-max      |                |          |              |        |

Table 1: The architecture of the WiseNet can be divided into two stages. The first one, in which an alternating combination of convolutional and max pooling layers are applied in order to extract low-level features. The second stage consists of three fully connected layers ending in a soft-max activation function.

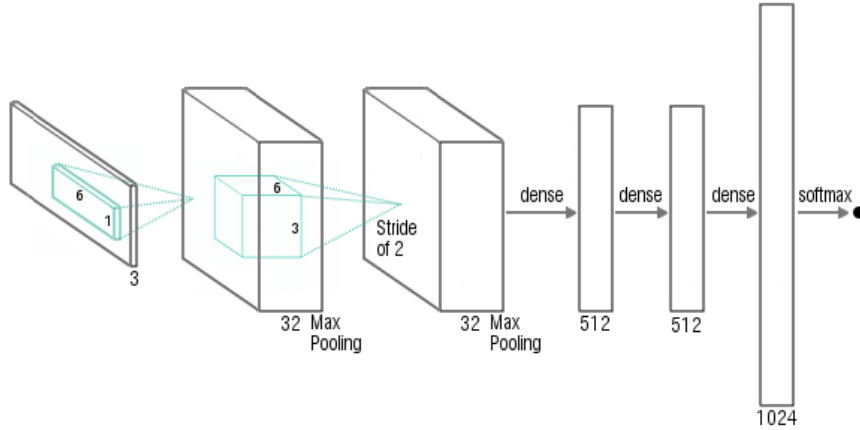


Figure 3: Schematic representation of the WiseNet architecture shown in Table 1. The convolution kernels applied in the first stage are shown colored in cyan.

## 4 EXPERIMENTAL RESULTS

In this section, we present the performance metrics of the image classification applied on the validation dataset described in Section 3. For the evaluation and comparison of models, we have used the following four different metrics with decreasing order of importance:

1. The Area Under the Curve (AUC).
2. The logarithmic likelihood of the classification (logloss).
3. The true positive fraction in the top-5% quantile (TP5).
4. The Brier score.

Whereas TP5 metric can be considered as one of the best metrics if we were to use the outcome of the model to optimize the detection and prevention of customer churn, we prioritize AUC as our main indicator, the reason being considered a more general metric because it takes into account not only the highest probabilities but all possible cutoffs.

Although the metrics used for performance evaluation of the models are the ones described previously, to select the best model in the training phase we took the one with the minimum log-loss in the

test dataset. By following this strategy, we expect to choose the least biased model and therefore the best one at generalizing. We show in Table 2 the WiseNet error, with a cutoff probability of 0.5, and log-loss of the best selected architecture evaluated in the three datasets: train, test and validation.

| Dataset    | Error  | Log-loss |
|------------|--------|----------|
| train      | 0.1967 | 0.4330   |
| test       | 0.1995 | 0.4273   |
| validation | 0.1979 | 0.4274   |

Table 2: Selected metrics of the best model on train, test and validation datasets. The small difference between these numbers indicates that the WiseNet model is performing with very little overfitting.

Besides the metrics shown in Table 2, the performance on the validation dataset of our main indicator (the AUC) is 0.8787, which can be considered generally as a good result for a binary classifier. The values of the remaining metrics are shown in Table 3. One remarkable aspect of the results shown in Table 2 is the really small difference in the log-loss between test and validation datasets. Although the difference is also small between the train set and the remaining two, it can be due to the fact that test and validation sets contain the same fraction of instances per class, whereas the training dataset is constructed as a balanced set. We also realized that the extensive use of dropout regularization layers had the effect of minimizing the overfitting of the model and improving generalization.

The framework we used for implementing the convolutional method is the publicly available cxxnet. Although this tool can be used natively as a distributed multi-GPU toolkit, due to the size of the problem we have not considered using multiple GPUs or a distributed GPU system at this moment. Therefore, our training stage was done in a single GPU machine equipped with one NVIDIA K20. A single manipulation is done by cxxnet previous to the training stage, the average image of the training dataset is calculated and then the value of every individual pixel in the image is subtracted to the mean.

#### 4.1 COMPARISON WITH OTHER MODELS

In order to compare our best WiseNet model with other machine learning techniques we used the same artificial images as comma-separated value (CSV) files. The information contained in the RGB channels was flattened into a single value per pixel and stored into CSV file. To maintain the information at the start-of-the-week mark, we added a new variable in the CSV which fills in this gap. This variable indicates the offset, in pixels, at which the random 4-week sample has been cropped. As a result, each customer was described by a feature vector of 1009 dimensions plus one extra column containing the class label.

We considered the performance of four well-known machine learning algorithms compared to the best performing WiseNet model: randomForests, generalized linear models (GLM), generalized boosted machines (GBM) and extreme gradient boosting (xgboost). We show on Table 3 the performance comparison for all models ranked by AUC in decreasing order from top to bottom. The optimal set of hyper-parameters was determined using the test dataset and optimizing the log-loss.

|              | AUC    | Log-loss | TP5    | Brier  |
|--------------|--------|----------|--------|--------|
| WiseNet      | 0.8787 | 0.4274   | 0.8929 | 0.1383 |
| xgboost      | 0.8561 | 0.4722   | 0.8908 | 0.1594 |
| GBM          | 0.8512 | 0.4995   | 0.8750 | 0.1662 |
| GLM          | 0.8228 | 0.6782   | 0.7592 | 0.2433 |
| randomForest | 0.8169 | 1.2482   | 0.8636 | 0.2018 |

Table 3: Validation metrics of the best model of each algorithm class. It can be noticed that WiseNets outperform all the other models in every indicator considered.

Looking at the results on Table 3, our WiseNet outperforms all the other models in every metric studied. Therefore, we can deduce that, under the conditions here reviewed, WiseNets can extract

a higher amount of information and learn specific feature representations. It can be noticed the relatively poor performance of the randomForest model, specially under the log-loss metric, because this model is optimized for minimizing misclassification error instead of log-loss. This particular model outputs a higher density of predictions in the top probability range  $p > 0.9$  when compared with other methods. This characteristic combined with the fact that its output is not particularly well calibrated in that probability range, as can be seen in Figure 4 b.5, damages the performance of its logarithmic loss score.

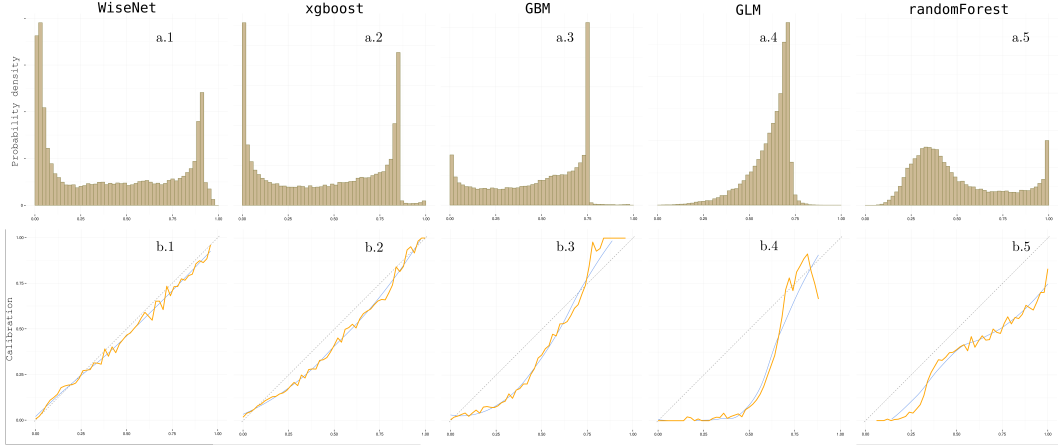


Figure 4: Probability density distributions and calibration curves of the models studied in this section. For the calibration curve, the orange curve represents the measured true positive rate for each probability step. A perfectly calibrated model would be represented as a straight line with a slope of 1. The blue curve is plotted as a guide and is just a smoothed version of the orange one.

#### 4.2 COMPARISON WITH FEATURE-ENGINEERING MODELS

Due to the lack of published literature about machine learning techniques applied to churn prediction in prepaid telecommunication networks, we present in this section a performance comparison between one of our in-house models which makes extensive use of feature engineering and a WiseNet. These features, developed and fine tuned during months of work, condense our knowledge of this particular market and its situation.

The in-house model has been trained with the same set of customers as previous models. It even includes new sources of data not used in the WiseNet model, such as the geographical location of customers, use of other mobile services, categorical variables and social relationships with other customers. Another significant difference with the WiseNet model is that the training dataset size of the feature-engineering model is larger but the same validation dataset has been used nonetheless.

|         | AUC    | Log-loss | TP5    | Brier  |
|---------|--------|----------|--------|--------|
| WiseNet | 0.8787 | 0.4274   | 0.8929 | 0.1383 |
| F-Model | 0.8552 | 0.4602   | 0.7184 | 0.1528 |

Table 4: Metrics comparison on the validation dataset between the WiseNet and the model using features (F-Model).

As we can see in Table 4, our WiseNet model outperforms the one using feature engineering in all the metrics considered, and this difference is particularly remarkable under the TP5 metric.

##### 4.2.1 COMPARISON WITH EXTERNAL MODELS FOR CHURN PREDICTION

There are several comprehensive reviews of the accuracy of customer churn predictive models in the telecommunication industry (Neslin et al., 2006) or in banking, retail and even insurance (Klepac

et al., 2014). Although the studied models do not target the same specific markets neither they have been measured using the same performance metrics as we have, we can compare the results that appear in Neslin et al. (2006) using their definition for the top-decile lift. In the best performing case studied by Neslin et al. (2006) the top-decile lift was 3.01, below the score of 3.52 that WiseNet achieves and far beyond the reported average of 2 units.

Burez & Van den Poel (2009a) reports a better lift performance of 4.4099 for a Logistic regression classifier applied to churn detection on a Mobile market but it underperforms WiseNet in AUC as it only scores 0.6785. Using text mining techniques, Coussement (2008) developed a classifier for predicting customer churn with a top-decile lift performance of 3.02 and an AUC of 0.7775, both figures underperform WiseNet metrics.

### 4.3 APPLICATION IN OTHER MARKETS

It can be conjectured that similar results can be achieved using the pre-trained WiseNet model in other markets, influenced by different factors. Inspired by this hypothesis, we evaluated the best WiseNet using data from other country and without re-training of the model, therefore using the same network architecture, weights and hyperparameters. The goal was to test the transferable property or generalization error of the model. We were surprised by the extremely good results obtained with this model (see Table 5). Two different reasons may justify this salient characteristic: (i) the customers’ behavior is similar in both countries and/or (ii) the model is capable of extracting general patterns which can be applied across different markets. The obtained probability density distributions and calibration curves are depicted in Figure 5. The effect of predicting without re-training can be appreciated in the calibration graph.

|                                 | AUC    | Log-loss | TP5    | Brier  |
|---------------------------------|--------|----------|--------|--------|
| trained WiseNet in market-1     | 0.8787 | 0.4274   | 0.8929 | 0.1383 |
| pre-trained WiseNet in market-2 | 0.8788 | 0.4449   | 0.9163 | 0.1428 |

Table 5: Metrics comparison on the validation datasets of two different markets. WiseNet model was learned using the train dataset of market 1 and tested using validation datasets of two different markets 1 and 2.

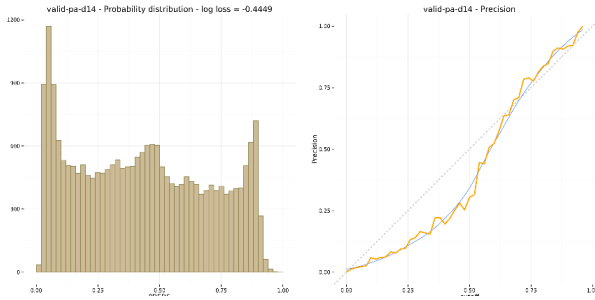


Figure 5: Probability density distributions and calibration curves of the WiseNet model applied to a different market without re-training (using the same network architecture, weights and hyperparameters).

### 4.4 LEARNED REPRESENTATIONS ANALYSIS WITH T-SNE EMBEDDINGS

In order to analyze the possible configurations associated with churn, we have applied a t-Distributed Stochastic Neighbor Embedding (t-SNE) to perform a dimensionality reduction on a subsample of 25 thousand users from the validation dataset. The input variables passed to the t-SNE are the states of the neurons in the last FC-1024 hidden layer. The results of the two-dimensional embedding can be seen in Figure 6.

On the left side of Figure 6, we can see the t-SNE embedding in which we have colored each point according to its probability of belonging to the churner class. It can be noted that despite not



including this probability among the inputs passed to the dimensionality reduction, there is a smooth distribution along the map of this variable. In particular, in the largest cluster of points, the churn probability seems to change almost continuously from one extreme to the other. The only exception is the one being delimited within the small square  $d$ .

Some of the most remarkable aspects of the left side of Figure 6 have been highlighted with labels  $a$  to  $d$ . As mentioned before, the probability across the largest cluster seems to change smoothly from the left green part to regions like  $a$  in which there is a high probability of churn. As this change is continuous, we can assume that the difference between these points is just quantitative, i.e. total call time or total amount of topups diminishes, but there is not a real qualitative change in phone activity usage. However, clusters like  $b$  and  $c$  are noticeably separated from the main cluster so there is a higher chance that they show a qualitative difference, rather than just a quantitative one, between the largest cluster. The location of the high-churn probability cluster  $d$ , completely embedded in a region of low churn probability, is quite a surprise. It could be due just to a simple convergence issue of the t-SNE algorithm or its location could have deeper foundations. Users in cluster  $d$  share an activity pattern similar to their non-churner neighbors but instead, they are labeled with a very high churn probability. More analysis would be needed in order to understand this situation as it could lead to a localized anomaly or to the discovery of a new activity pattern.

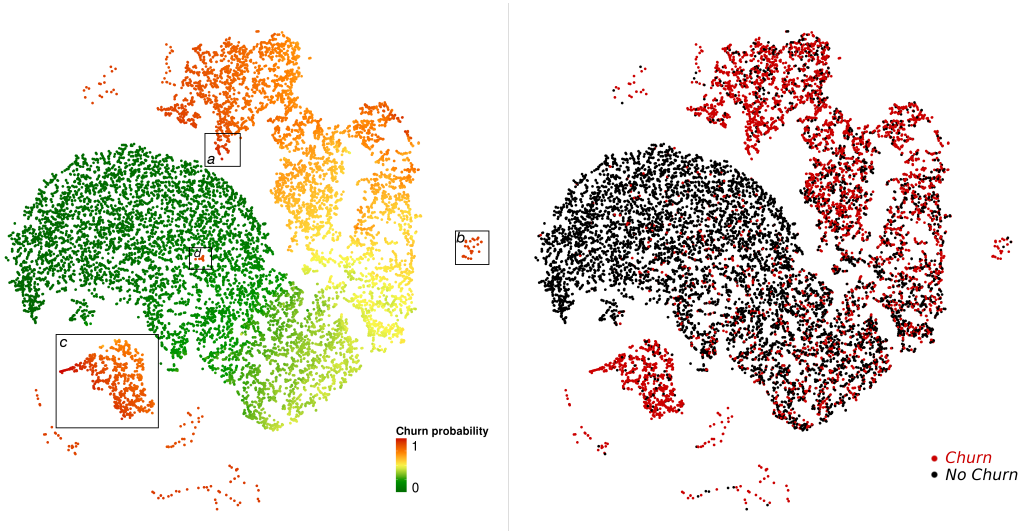


Figure 6: Two dimensional t-SNE embedding of the validation dataset using the states of the 1024 neurons of the last hidden layer. On the left image, each point is colored according to the probability given by the WiseNet for each user belonging to the churner class, red corresponds to the highest probability and green the lowest. On the right image the color corresponds to the observed class with red being a churner.

Another singular feature of the t-SNE embeddings is that there are no isolated clusters with low-churn probability, other than the largest one. We could interpret this as different causes for customers to churn from the service provider e.g., bad network coverage, expensive costs. . . etc. but the reason to stay can be summarized as a simple cause, e.g. the customer needs and wants the service.

## 5 SUMMARY AND CONCLUSIONS

Nowadays, machine learning engineers spent most of their time finding good representations for their models and a huge research effort is done trying to come up with better features.

In this work we investigated the application of ConvNets trained with GPUs to build better predictive models in telecommunication business environments and developed the WiseNet model. For the particular problem that we considered, it has been shown that WiseNet outperforms commonly used machine learning models using the same input data. We have also shown that it is possible to

automatically learn the representations required for a specific business problem, providing more accurate predictions than traditional machine learning models built with hand-crafted features. This finding is translated into an exponential decrease in the required human-effort for feature engineering compared to traditional machine learning models.

Furthermore, similar results were achieved using the pretrained WiseNet model in other markets, which may be influenced by different factors. So, we confirmed the generalization property of the WiseNet model and its ability to discover useful representations. As an ongoing work we are applying the WiseNet model to other prediction tasks with promising preliminary results.

We have also experimented with an extended data representation and network model, however due to the confidentiality restrictions we are not allowed to disclosed them to the public.

## ACKNOWLEDGEMENTS

We would like to thank Alfonso Vazquez for his valuable comments and insights to develop this work.

## REFERENCES

- Bengio, Yoshua, Courville, Aaron, and Vincent, Pierre. Representation learning: A review and new perspectives. *IEEE Transactions on Pattern Analysis and Machine Intelligence*, 35(8):1798–1828, 2013.
- Burez, J. and Van den Poel, D. Handling class imbalance in customer churn prediction. *Expert Systems with Applications*, 36:4626–4636, 2009a.
- Burez, Jonathan and Van den Poel, Dirk. Handling class imbalance in customer churn prediction. *Expert Systems with Applications*, 36(3):4626–4636, 2009b.
- Coussement, K. Employing sas text miner methodology to become a customer genius in customer churn prediction and complaint e-mail management. In *SAS Global Forum*. SAS, 2008.
- Glorot, Xavier and Bengio, Yoshua. Understanding the difficulty of training deep feedforward neural networks. In *International conference on artificial intelligence and statistics*, pp. 249–256, 2010.
- He, Kaiming, Zhang, Xiangyu, Ren, Shaoqing, and Sun, Jian. Delving deep into rectifiers: Surpassing human-level performance on imagenet classification. *arXiv preprint arXiv:1502.01852*, 2015.
- Hinton, Geoffrey E., Osindero, Simon, and Teh, Yee Whye. A fast learning algorithm for deep belief nets. *Neural Computation*, 18:1527–1554, 2006.
- Huang, Bingquan, Kechadi, Mohand Tahar, and Buckley, Brian. Customer churn prediction in telecommunications. *Expert Systems with Applications*, 39(1):1414–1425, 2012.
- Karpathy, Andrej, Toderici, George, Shetty, Sachin, Leung, Tommy, Sukthankar, Rahul, and Fei-Fei, Li. Large-scale video classification with convolutional neural networks. In *IEEE Conference on Computer Vision and Pattern Recognition (CVPR)*, pp. 1725–1732. IEEE, 2014.
- Klepac, G., Kopal, R., and Mršić, L. *Developing Churn Models Using Data Mining Techniques and Social Network Analysis*. IGI Publishing, 2014. ISBN 1466662883.
- LeCun, Yann, Kavukcuoglu, Koray, and Farabet, Clément. Convolutional networks and applications in vision. In *Proceedings of 2010 IEEE International Symposium on Circuits and Systems (ISCAS)*, pp. 253–256. IEEE, 2010.
- Luciano, Patrick, Rebai, Ismail, and Lemaire, Vincent. Increasing loyalty using predictive modeling in business-to-business telecommunication. *CoRR*, abs/1506.03214, 2015. URL <http://arxiv.org/abs/1506.03214>.
- Mikolov, Tomas, Chen, Kai, Corrado, Greg, and Dean, Jeffrey. Efficient estimation of word representations in vector space. *arXiv preprint arXiv:1301.3781*, 2013a.

- Mikolov, Tomas, Sutskever, Ilya, Chen, Kai, Corrado, Greg S, and Dean, Jeff. Distributed representations of words and phrases and their compositionality. In *Advances in neural information processing systems*, pp. 3111–3119, 2013b.
- Neslin, S. A., Gupta, S., Kamakura, W., Lu, J., and Mason, C. H. Defection detection: Measuring and understanding the predictive accuracy of customer churn models. *Journal of Marketing Research*, XLIII:204–211, May 2006.
- Richter, Yossi, Yom-Tov, Elad, and Slonim, Noam. Predicting customer churn in mobile networks through analysis of social groups. In *SDM*, volume 2010, pp. 732–741, 2010.
- Senior, Alan, Heigold, Georg, Ranzato, Marc’Aurelio, and Yang, Ke. An empirical study of learning rates in deep neural networks for speech recognition. In *Acoustics, Speech and Signal Processing (ICASSP), 2013 IEEE International Conference on*, pp. 6724–6728. IEEE, 2013.
- Simonyan, Karen and Zisserman, Andrew. Two-stream convolutional networks for action recognition in videos. In *Advances in Neural Information Processing Systems*, pp. 568–576, 2014.
- Simonyan, Karen and Zisserman, Andrew. Very deep convolutional networks for large-scale image recognition. *arXiv preprint arXiv:1409.1556*, 2015.
- Srivastava, Nitish, Hinton, Geoffrey, Krizhevsky, Alex, Sutskever, Ilya, and Salakhutdinov, Ruslan. Dropout: A simple way to prevent neural networks from overfitting. *The Journal of Machine Learning Research*, 15(1):1929–1958, 2014.
- Szegedy, Christian, Liu, Wei, Jia, Yangqing, Sermanet, Pierre, Reed, Scott, Anguelov, Dragomir, Erhan, Dumitru, Vanhoucke, Vincent, and Rabinovich, Andrew. Going deeper with convolutions. *arXiv preprint arXiv:1409.4842*, 2014.
- Wilson, Jobin, Kachappilly, Chitharanj, Mohan, Rakesh, Kapadia, Prateek, Soman, Arun, and Chaudhury, Santanu. Real world applications of machine learning techniques over large mobile subscriber datasets. *CoRR*, abs/1502.02215, 2015. URL <http://arxiv.org/abs/1502.02215>.
- Yoon, Sangho, Koehler, Jim, and Ghobarah, Adam. Prediction of advertiser churn for google ad-words. In *JSM proceedings*, 2010.